

PAPER • OPEN ACCESS

Immobilised Gold Nanostructures on Printing Paper for Lable-Free Surface-enhanced Raman Spectroscopy

To cite this article: Rawaa A. Faris *et al* 2020 *IOP Conf. Ser.: Mater. Sci. Eng.* **871** 012019

View the [article online](#) for updates and enhancements.

You may also like

- [Fabrication of low cost highly structured silver capped aluminium nanorods as SERS substrate for the detection of biological pathogens](#)
Sathi Das, Laxman Prasad Goswami, Jampana Gayathri et al.
- [Fabrication of antireflective silver-capped tin oxide nano-obelisk arrays as high sensitive SERS substrate](#)
Abdul Rasheed Paloly and M Junaid Bushiri
- [Silver nanodendrites for ultralow detection of thiram based on surface-enhanced Raman spectroscopy](#)
Ashwani Kumar Verma and R K Soni



ECS
The
Electrochemical
Society
Advancing solid state &
electrochemical science & technology

DISCOVER
how sustainability
intersects with
electrochemistry & solid
state science research

Immobilised Gold Nanostructures on Printing Paper for Label-Free Surface-enhanced Raman Spectroscopy

Rawaa A. Faris¹, Zainab F. Mahdi¹ and Mohammad D. Abd. Husein²

¹ Institute of Laser for Postgraduate Studies, University of Baghdad, Baghdad, Iraq

² Al-Yarmouk Teaching Hospital, Baghdad, Iraq

E-mail: rawaa@ilps.uobaghdad.edu.iq

Abstract :

In this research, paper-based SERS active substrates with different grade gram per square meter (GSM) were prepared by adsorbing 40 nm spherical GNP and 40nm star shaped gold nanostructures GNS. Besides the SERS evaluation and optimization, morphological parameters of the samples were found to strongly affect the enhancer properties of the substrates. The developed substrate was tested regarding surface homogeneity as well as by the Raman reporter dye Methylene Blue (MB). These paper-based SERS active substrates are simple to prepare, easy to handle and cheap solid SERS substrates. GNS with 135 GSM printing paper can be easily used as highly active SERS active substrates, with average enhancement factor $EF = 10^5$.

1. Introduction:

Surface Enhanced Raman Spectroscopy (SERS) is point of use, a label-free spectroscopic technique showing high selectivity, sensitivity based on molecular fingerprinting, and even at single-molecule detection levels. SERS based sensor with applications in a wide variety of bioanalytical or material characterization settings has been developed. The SERS technique requires adsorption of the analyte molecules onto the SERS substrate. The high resolution of the SERS spectra makes simultaneous multicomponent analysis possible. In addition, molecules adsorbed to the surface of gold nanostructured appear the SERS effects, due to the coupling of the SPR band of the gold nanostructure with the molecules' electronic states of analyte ¹⁻⁴.

Paper-based SERS substrate has advantages such as low cost, ease of fabrication, demonstrates both high-sensitivity and great reproducibility, making it a platform for applications in fields such as food safety, forensic science, and environment protection.

For typical on-field SERS diagnostic applications, the optimized nanostructures need to be assembled over a flexible substrate. Paper is the preferred choice of substrate as it is affordable, biodegradable and easily disposable by incineration ⁵. Techniques used for patterning metal nanostructures on the paper include pen on paper ⁶, self-assembly, ⁷ filtration, ⁸ dip-coating, ⁹ screen-printing, ¹⁰ inkjet printing.

The unique properties of paper such as flexibility, hydrophilicity are well suited for analysis of samples with trace level as well as those that can be easily transferred to lab.



Printing nanostructures onto the paper are a rapid and low cost technique for fabrication of paper-based SERS substrate^{11,12,13}

Most researches used filter paper, chromatography paper or inkjet printing paper as the substrate material for various paper based SERS applications, including a Pen on Paper scheme where plasmonic nanostructures have drawn and immobilized on the paper. Both types of paper constituted by cellulose with small differences in composition and surface chemistry between them¹⁴.

Because the morphology of metal nanostructures determines their local electric field distribution and thereby the SERS efficiency, various morphologies have been studied for optimization and evaluation of SERS signals. Amongst different morphologies, gold nanostars (GNS) with multiple branches and sharp tips that serve as SERS “hotspots” have showed higher SERS enhancement factors (EF) compared to nanoparticles and nanorods^{15,7}.

So, the objective of this study was to investigate the effect of GSM grade of printing paper on the EF of SERS with Gold nanostructure(GNP&GNS).

2. Materials and Methods

2.1. Sample preparation

The general technique adapted to prepared gold nanostructures immobilized printing paper-based SERS substrate for the quantification of MB concentration is summarized as follows:

Stage 1- Sample preparation: A series of standard solutions (i.e. solutions in which the MB concentration is accurately known) was prepared. MB ($C_{16}H_{18}ClN_3S \cdot 3H_2O$) was purchased from Sigma-Aldrich with the molar weight of 373.90 g/mol. It is a water soluble powder.

Aqueous solution of MB with a high concentration of 0.063 M was prepared and then, new concentrations were prepared (0.063M, 0.063mM, 0.063 μ M, 0.063 nM).

Stage 2- Mixture preparation: gold nanostar GNS and gold nanoparticles GNP were purchased from Nitparticles, Spain.

Mixture of 89 vol% of the GNP (0.11 nM) and GNS (0.20 mM)solutions , 1 vol% sodium chloride solution (20 mM) and 10 vol% analyte solutions MB were mixed for ten min and then used for the SERS measurements on paper strips, 5 mL of mixture solution were dropped onto the paper strips and dried at room temperature.

Stage 3- a proper substrate, which are printing papers with different GSM were used (120,135,160,180,240,260) GSM (Double A, Singapore) have been used to evaluated the performance of the proposed paper based SERS substrate. Each paper substrate has a dimension of 2 cm x 3 cm.

2.2. Surface Enhanced Raman Scattering (SERS) measurements

A Holmarc (HO-ED-S06) laser Raman spectrometer is utilized for Raman measurement. The excitation source is emitting a 11 mW at 532 nm Diode Pumped Solid State (DPSS) laser. Raman spectra are acquired in a 45° scattering with an objective of 0.09 Numerical apertures (NA). SERS measurements of MB are performed from three different places across the whole nanostructured area and the averaged value is adopted. The Raman spectra of MB are region of organic molecules is generally considered to be in the range from 500-2000 cm^{-1} and the exposure time 10s.

2.3. Sample Characterization Measurements

The GNPs and GNS embedded in paper substrate were analyzed using MIRA3 (Czech Republic) which is high performance FESEM system which features a high brightness Schottky emitter for achieving high resolution and low-noise imaging.

Topographic AFM examinations were performed by using a Nanoscope IIIa contact-mode Microscopy (AFM, modal AA 3000 scanning probe microscope from Angstrom Advanced Inc., USA). It was used to find the average particles size and surface roughness of the samples. The GNPs and GNS were characterized using JEOL JEM-2011 (Jeol LTD, Tokyo, Japan) transmission electron micrographs (TEM) in order to measure the size and the morphology of gold nanostructures.

3. Results and Discussion:

3.1. SERS Results:

According to figure 1(a,b) it can be seen that, only a part of Raman bands are recognized, such as at 449, 499, 1399, 1478 and 1630 cm^{-1} . Both the bands at 449 and 499 cm^{-1} are belonged to C-N-C skeletal bending vibrations.

Among many SERS substrates that produced during this study, the SERS substrate of 40 nm gold nanostar on 135 GSM and 40 nm gold nanoparticle on 240 GSM gives the strongest enhancement effect and are elected here for detection of MB traces in water as shown in Figures (1,2).

It exhibits the SERS spectra of MB adsorbed on the substrate with a concentration ranging from 0.063 M down to 0.063 nM. In comparison with normal Raman spectrum of methylene blue aqueous solution figures.1,2, good quality and high well-resolved SERS spectra are achieved for MB adsorbed on the substrate where the characteristic bands of MB at 449, 499, 1399, 1478 and 1630 cm^{-1} are recognized

at concentration as low as 0.63 nM. The major bands of SERS and normal Raman scattering of MB are consistent where there are no blue or red shift detected in the SERS of MB but there are an alterations in the relative intensities of the characteristic bands of SERS in comparison with normal Raman scattering. These relative intensities alterations of characteristic bands are belonged to interaction of MB molecules with active metal surface ^{8,10}.

The concentration of the probe molecule is proportional to its Raman peak intensities. When we acquire Raman spectra from our samples, which are MB in solid state or MB aqueous solutions, we know that the observed signal originates from MB. Therefore, we can consider that the LOD of MB corresponds with the LOD of its most intense Raman peak, which is located at a Raman shift of 1630 cm^{-1} as can be seen in figures. 1,2 . Therefore, we can apply a univariate analysis using the MB peak intensity at 1630 cm^{-1} , which is assigned to (C-C) ring stretching and (C-N) ring stretching according to Table(1) , as a criterion to estimate the MB concentration. Since the peak at 1630 cm^{-1} is the strongest MB Raman peak at the excitation wavelength of 532 nm, this peak is more detectable compared to the other MB Raman peaks in the diluted samples. Therefore, selecting this peak as our key feature leads to a very low LOD of MB.

Table 1. Experimentally observed vs. reported MB aqueous solution Raman peaks and their theoretical assignments.

Experimentally observed MB aqueous solution Raman peaks	Reported MB Raman peaks	Band assignment
449	450 (w)	$\alpha (C - N - C)_{AMG}$
499	500 (w)	$\alpha (C - N - C)_{AMG}$
1399	1390 (s)	$\nu (C_9-N_{10})$; $\nu (C_3-N_2)$; $\nu (C - N)_{Ring}$; $\beta(CH)$
1630	1625 (vvs)	$[\nu (C - C); \nu (C - N)]_{Ring}$

vvs: very very strong; s: strong, w: weak, ν : stretching; AMG: Attached to Methyl Group.

(a)

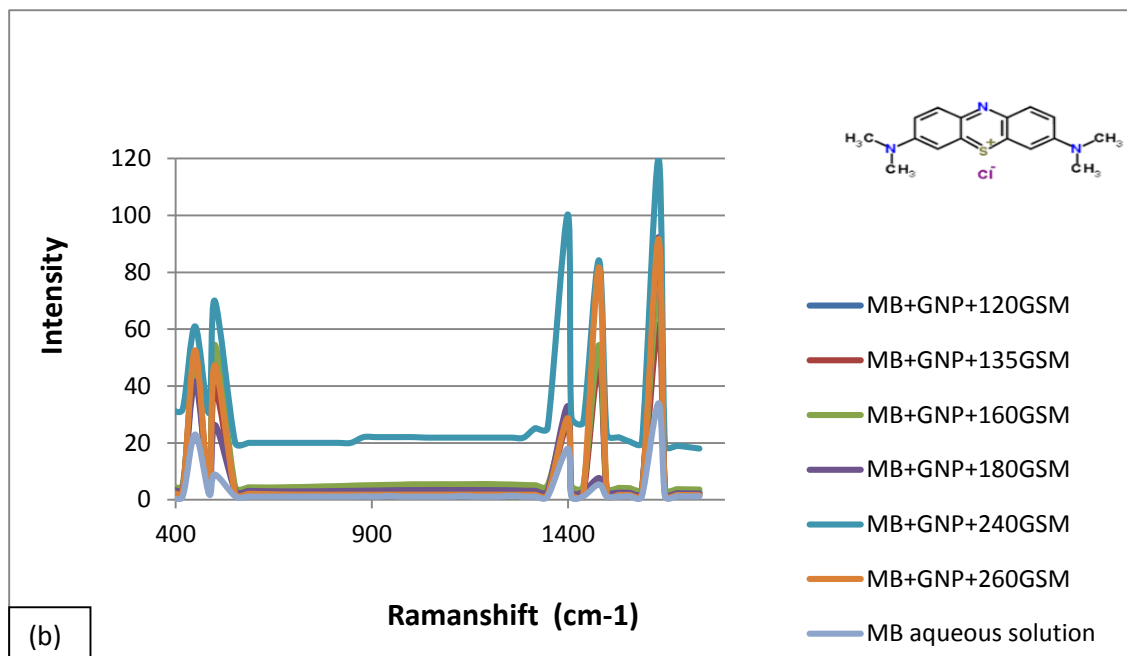


Figure 1: (a) Chemical structure of MB, (b) Raman spectrum of MB aqueous solution and for MB and GNPs(40 nm) on printing papers with different grade GSM(120,135,160,180,240,260), (Excitation wavelength: 532 nm, Exposure time:10s.

As SERS from plasmonic nanostructures originates predominantly from electromagnetic enhancement and to a lesser extent from chemical enhancement, the sharp spikes on GNS were morphological features with a strong localized electromagnetic field and thus served as SERS “hot spots” which can be seen in fig.(2).

Studies have shown that GNS exhibited a higher SERS enhancement both in colloid and after immobilization on paper substrate compared to gold nanospheres or gold nanorods^{3,5,9,10}.

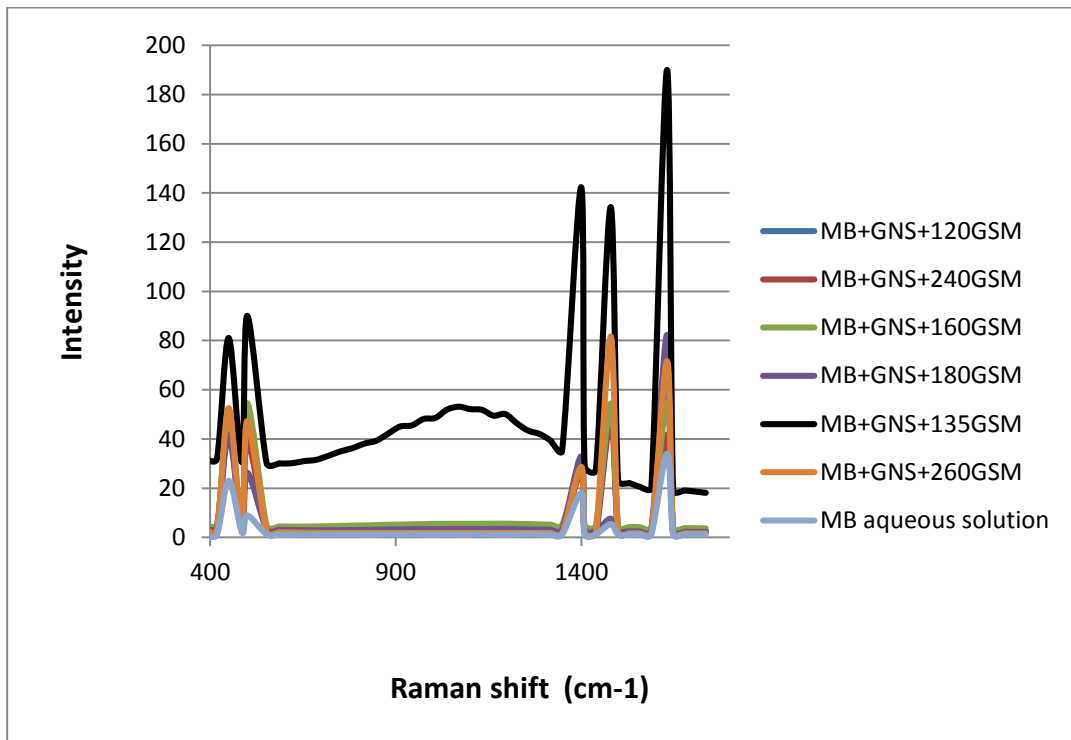


Figure 2: Raman spectrum of MB aqueous solution and for MB and GNS(40 nm) on printing papers with different grade GSM(120,135,160,180,240,260), (Excitation wavelength: 532 nm, Exposure time:10s.

To quantify the corresponding enhancing performance for the paper substrate which was achieved under above mentioned optimal conditions, MB was used to calculate the enhancement factor (EF), which was given by the following formula²:

$$EF = (I_{SERS}/C_{SERS}) / (I_{RS}/C_{RS}) \quad \dots\dots\dots(1)$$

Where I_{SERS} and I_{RS} are the intensities of 1630 cm^{-1} of MB for SERS and conventional Raman spectra (see Figure 3) and C_{SERS} and C_{RS} are the concentrations of MB molecules SERS and Raman measurement.

An average EF of 50×10^5 was achieved under this optimized condition for the GNS on 135 gsm printint paper and 45×10^5 and for the GNPs on 240 gsm printint paper.

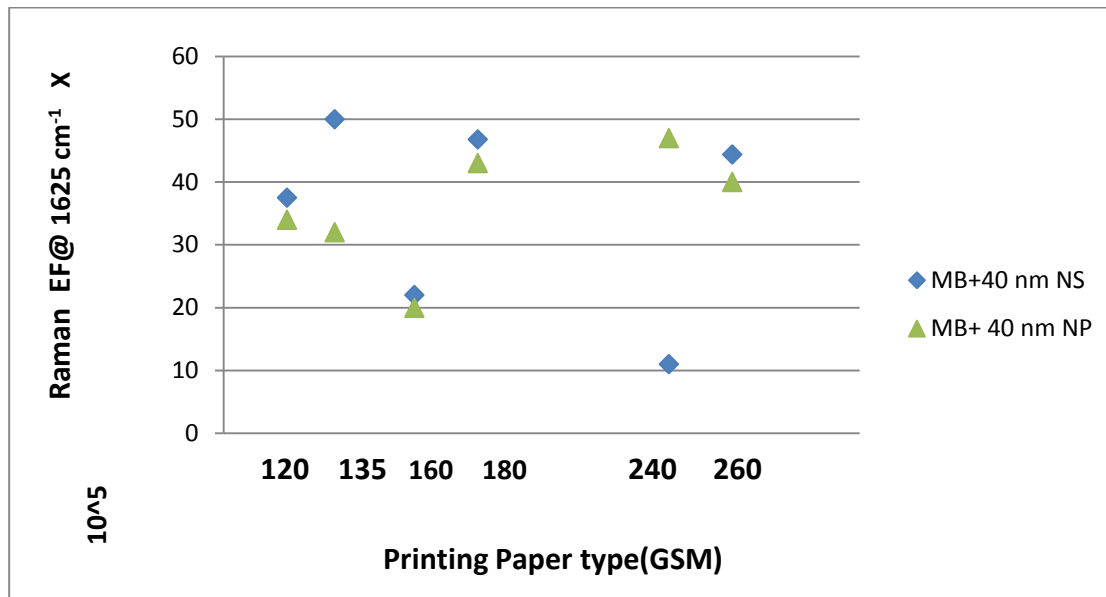


Figure 3: Raman enhancement factor of MB and GNS(40 nm) and GNP(40 nm)on printing papers with different grade GSM(120,135,160,180,240,260)

Significantly, in all measurements made, as shown in Figure 3, the magnitude of the SERS response was highest for the gold nanostars and lower for the aggregated Nanospheres except for GNP with 240 GSM . The results are consistent with the requirement for enhanced electric fields at hotspots associated with aggregated nanospheres, or the vertices of star shaped nanoparticles.

The fundamental process of SERS is based on the local field enhancement in the region of metallic nanostructures upon excitation of the SPR.

However, aggregation is not a well-controlled phenomenon and adds further uncertainty and variability to an already complex system. An alternative way to increase the local electromagnetic field associated with the SPR is to increase the local curvature of nanomaterials. It has been shown that when two spherical nanoparticles are aggregated or close enough, the SPR band is split into two components: longitudinal (low frequency) and transverse (high frequency). In spherical particles, these two modes (quadrupole and dipole) are not distinguishable from one another. In the case of nanotriangles, due to their anisotropic shape, four different plasmon resonances have been observed: inplane dipole, quadrupole, out-of-plane dipole, and quadrupole. Nanostars contain a higher number of sharp corners and edges, and they have their own unique character as more complex anisotropically shaped nanoparticles and the modes oscillate at markedly different frequencies in Au materials⁵.

3.2. Characterization of SERS Substrate:

An ideal SERS-active substrate requires a uniform distribution of nanostructures to achieve reproducible measurements. FESEM images in Figure 4 (a) were shown the distribution for GNP on 240 GSM printing paper, GNPs formed a sparse and uneven distribution, and few clusters were observed or nanoclusters were more uniformly distributed on paper surface. Figure 4 (b) Represented more ordered and uniform distribution for GNS on 135 GSM printing paper, thus enabling high-performance SERS detection as can be seen in figure.3.

TEM image conformed the spherical shape of nanoparticles as can be seen in the lower of Fig.4a which shows GNPs (40nm) are uniform quasi spherical with a mean diameter of forty nanometers capped with citrate. In the lower of the Fig.1b represents TEM image for gold nanostars which are uniform in star shape. GNS comprises a spherical inner core with multiple branches and sharp tips with a mean diameter of forty nanometers capped with Poly vinyl pyrrolidone.

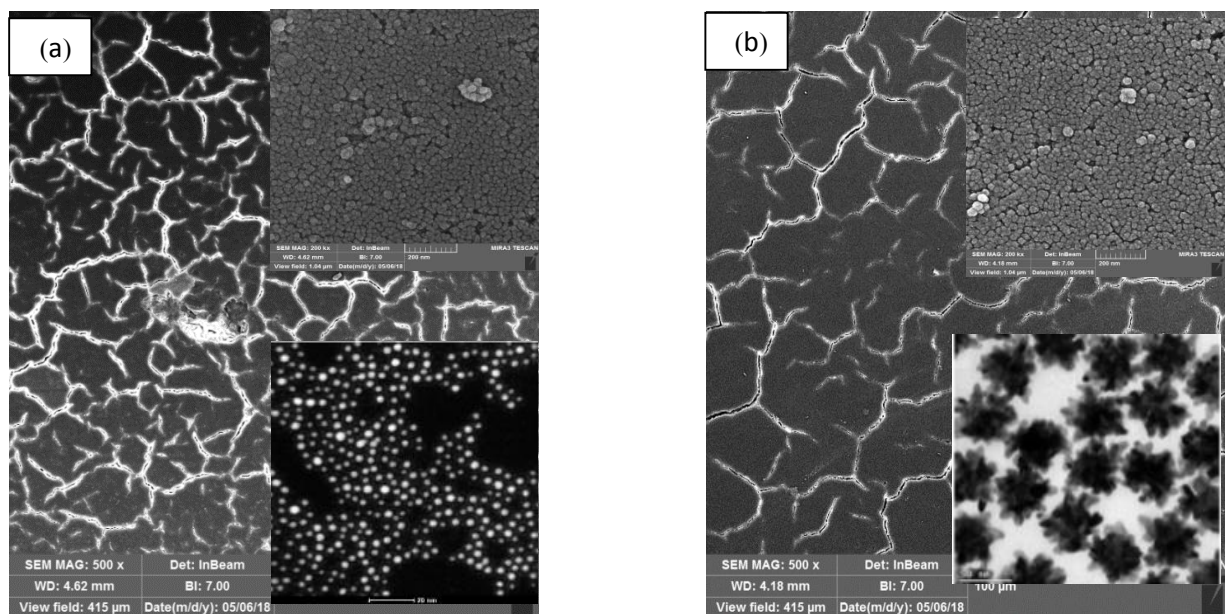


Figure 4: FESEM images of (a) GNPs on printing papers (240 GSM), (b) GNS on printing papers (135 GSM). (The magnification for the upper image is 200,000 times and the scale bar is 200 nm, and for the lower image the magnification is 5,00 times and the scale bar is 100 μm).

Lower image in (a) is the TEM image for GNPs and the lower image in (b) is the TEM image for the GNS.

The surface morphology of paper and gold nanostructures were studied by AFM.

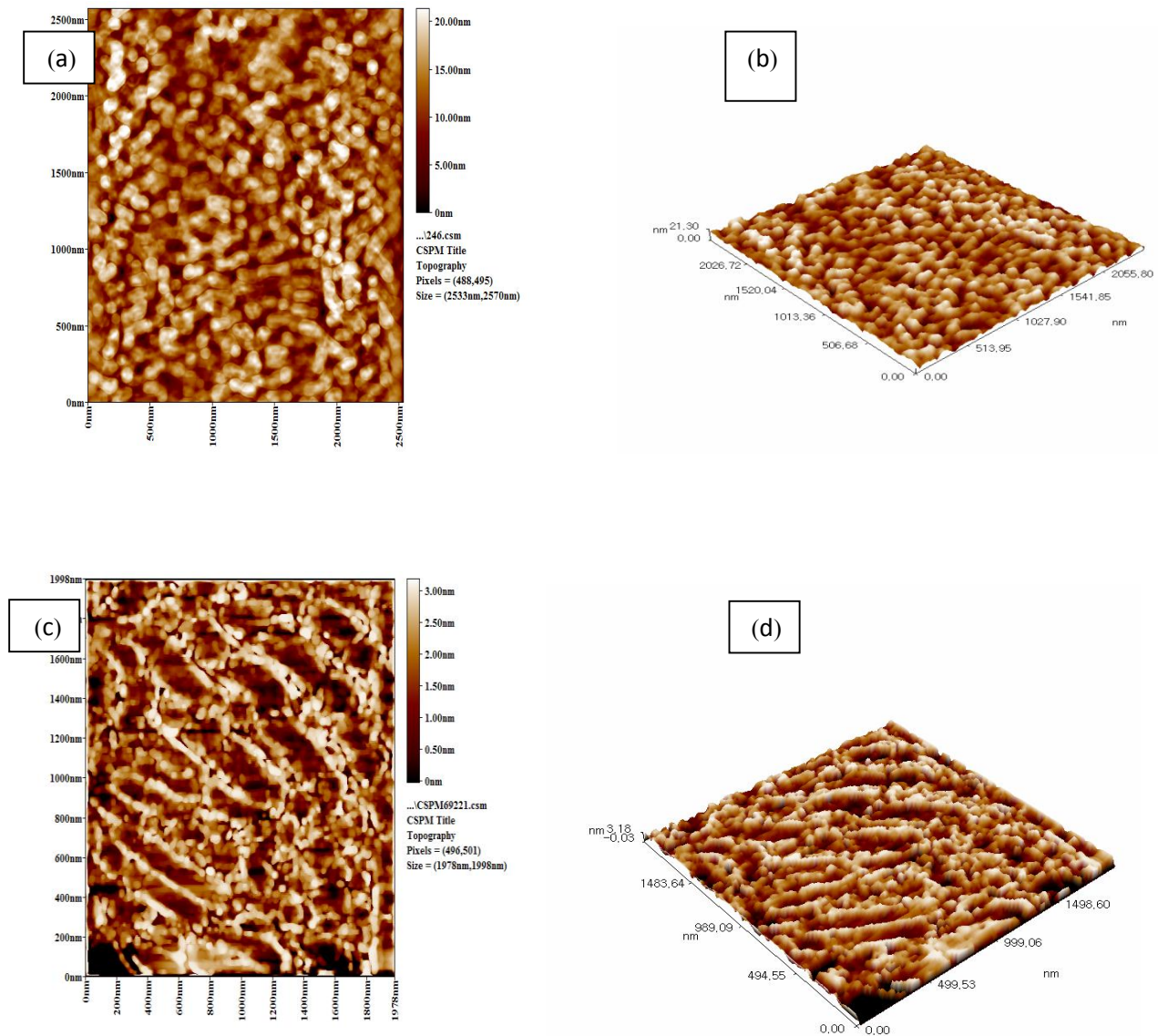


Figure 5: AFM images of (a)GNPs on printing papers 240 gsm (2D), (b)GNPs on printing papers 240 gsm (3D) (c) GNS on printing papers 135 gsm(2D), (d) GNS on printing papers 135 gsm(3D)

Figs. 5(a,b) show the random distribution of GNPs on printing papers 240 gsm while figs. 5(c,d) show a uniform distribution of the GNS on printing papers 135 gsm with deep grooves on the trajectory of the moving particles. This result comes from the gold nanostar structure which arranges in an array manner (periodic surface structures) which affected the Raman spectrum of this sample and then gives higher EF. The incident laser light interferes with a wave scattered off the sample surface, initially

produced due to the natural roughness of surface, which results in a heterogeneous light intensity distribution on the surface. The ripples having these properties are usually referred to as low spatial frequency. Recently, a new kind of ripples has been observed with a periodicity larger than the laser wavelength. These ripples usually look like a "grooves". The GNS on printing papers 135 gsm have good raman properties with very low cost compared with other methods to have ripples such as Laser Induced periodic Surface Structure (LIPPS) which is expensive, time consuming and inefficient for large scale substrates[8].

4. Conclusions:

The results of this research have demonstrated that for paper SERS substrate with colloidal GNPs and GNS which have a great impact on SERS performance, that was explained in detail with the corresponding FESEM, AFM images of GNS on the paper substrate. The individual particles or fluffy particle aggregates captured by ionic forces (chloride) on the cellulose-based 3D structure offer a relatively clean and high specific area noble metal surface for the analyte molecules. The good Raman enhancer properties, unique mechanical features, simple and cheap preparation process of this paper based substrates suggest that these materials might contribute to the development of more economic, convenient and user friendly SERS based methods for various analytical problems.

5. References

- [1] Pushkaraj, J. ; Venugopal, S. ,2016, *RSC Adv.*, **6**, 68545–68552
- [2] Pamela, A., *Nanomaterials*, 2017, Review of SERS Substrates for Chemical Sensing, s, **7**, 142.
- [3] Anirban, D. ; Sourav, P. ; Sandip, B. ; Goutam, D., 2013, *J Nanopart Res.* , **15**:1804.
- [4] Pushkaraj, J. ; Venugopal, S., 2018, *Industrial & Engineering Chemistry Research* , **4**
- [5] Zufang, H.; Gang, C.; Yan, S. ; Shengrong, D.; Yongzeng, Li; Feng, S.; Juqiang, L; Jinping, L., 2017, *Journal of Nanomaterials* , Vol. **4**, 8.
- [6] Shuai, H.; Jefri, C.; Eddie, K. M. ; James, C.; Yong, K. ., 2017, *The Royal Society of Chemistry* , **7**, 16264–16272
- [7] Nalbant, E., 2009, *J. Raman Spectrosc.*, **40**, 86–91
- [8] Tian, F., 2014, *Analytical Methods*, **6**, 9116-9123
- [9] Axel, B.; Ulrich P.; Knut R.; Merwe B. , 2016, , *Anal. Methods*, **8**, 1313–1318.
- [10] Dora, M.; Carlo M.; Renzo V.; Marzia B.; Davide P.; Furio G., 2013, *Vibrational Spectroscopy*, **68**, 45–50
- [11] Mosier-Boss P. , *Nanomaterials* , 2017, **7** (6), 142.
- [12] Betz, J. F.; Yu, W. W.; Cheng, Y.; White, I. M.; Rubloff, G. W. , *Phys. Chem.* , 2014, **16** (6), 2224.

- [13] Yang, Y.; Matsubara, S.; Xiong, L.; Hayakawa, T.; Nogami, M. Solvo, , *J. Phys. Chem. C* , 2007, 111 (**26**), 9095.
- [14] Bell, S. E. J.; McCourt, M. R. ,. *Phys. Chem.* , 2009, 11 (**34**), 7455.
- [15] Hao, E.; Schatz, G. C. , *J. Chem. Phys.* , 2004, 120 (**1**), 357.